Dept. of Mech. Eng.
CUET

Published Online April 2017 (http://www.cuet.ac.bd/merj/index.html)

Mechanical Engineering Research Journal

Vol.10, pp. 14-19, 2016

ISSN: 1990-5491

NUMERICAL MODELING OF TURBULENT FLOW THROUGH BEND PIPES

R. R. Chowdhury[1*], M. M. Alam[2] and A. K. M. Sadrul Islam[3]

[1-2]Department of Mechanical Engineering, CUET, Chittagong, 4349, Bangladesh
[3]Department of Mechanical and Chemical Engineering, IUT, Gazipur, 1704, Bangladesh

Abstract: A numerical investigation has been carried out for incompressible turbulent flow through 90^0 bend pipes. The model is based on the numerical solution of conservation equations of mass and momentum. The numerical results are validated against existing experimental results. Then, the results of the simulations of the flow in the form of contour and vector plots for two types of pipe bend both mitre and smooth bend with seven different Reynolds numbers (2.0+E04, 2.5+E04, 3.0+E04, 3.5+E04, 4.0+E04, 4.5+E04 and 5.0+ E04) are presented in this paper. From the obtained results, it is seen that the mitre bend pipes produces more turbulent kinetic energy, eddy viscosity and skin friction factor compared to that of the smooth bend pipes. To further investigation on smooth bend pipes, the static pressure distribution along the inner, outer wall and the pressure loss factor with different Re numbers are analyzed for different R/D ratios. However, it is noticed that as Re increases the pressure gradient changes rapidly at the inner and also the outer wall of the bend. Again, the total pressure loss factor (k_l) increases as the R/D ratio decreases and due to higher velocity heads, factor k_l decreases as Re increases.

Keywords: *Turbulent flow, Turbulent kinetic energy, Eddy viscosity, Skin friction factor, Pressure loss factor.*

NOMENCLATURE

Symbol	Meaning	Unit
$\vec{V}$	Velocity vector	(m/s)
k	Turbulence kinetic energy	(J/Kg)
ε	Eddy viscosity	(Pa)
u_{avg}	Average velocity	(m/s)
ρ	Density	(Kg/m^3)
υ	Kinematic viscosity	(m^2/s)
R	Radius of curvature	(m)
D	Diameter	(m)
B	Breadth	(m)
Re	Reynolds number	Dimensionless

1. INTRODUCTION

Various researches had been carried out to study the flow phenomena of bend pipes in experimentally and numerically. CFD technique is widely used to analyze the flow characteristics of a bend pipe. The researchers still work on this topic to know about secondary flow, the pressure, velocity variations along the inner and outer walls of the bend pipes. In addition to that, researchers want to conclude the effect of curvature ratio on flow phenomena and flow accelerated corrosion analysis for different engineering purposes [1, 2].

Some of the major applications include oil and gas production field with their distribution networks, the energy conversion systems found in same design of nuclear reactor, heat exchangers, solar collectors, components of internal combustion engines (e.g. exhaust manifolds) and cooling of industrial machines and electronic components [5,9]. As Bangladesh is approaching to the era of nuclear power generation, in future this paper can be used for flow measurement and FAC (flow accelerated corrosion) rate analysis for the bend under high pressure and temperature where the difficulties arise on due to the restriction of reactor structure and wicked measuring environment [6,7].

When a fluid flows through a bend it causes the fluid particles to change their motion. The secondary flow generated from the curvature is superimposed on the primary flow. In addition to that, the strong action of centrifugal force produces higher wall pressure in the outer wall and reverse is occurred in the inner wall side of the bend. Thus, the fluid experiences an adverse pressure gradient at bend and this disturbance of flow exists further downstream of the bend [3].

The aim of this paper is to compare the flow phenomena

* **Corresponding author:** Email: engr.rrc@gmail.com; Tel: 880-1818141816

between mitre and smooth bend, then to analyse the effect of curvature ratio i.e. R/D ratio on the smooth bend with different Re numbers.

2. SOLUTION METHODOLOGY

The mass and momentum equation with the standard k-ε model has been adopted for the computation of turbulent flow through the bend pipes. The ANSYS-FLUENT software is used and allowing a 3D analysis for the solution of the present problem. The SIMPLE algorithm which is based on a finite volume discretization of the governing equations as suggested by Patankar (1980) is used for numerical modeling [6]. A spatially second-order upwind scheme for the flow equations and fluent's "standard" scheme for the pressure is used for discretization purpose. The Three-dimensional unstructured mesh is used which is containing tetrahedral and wedges as control volumes in the entire fluid domain. Thus, the meshing of the geometry is accomplished through Ansys meshing application by setting the element size 6e-3 and changing the inflation mode into program controlled.

2.1 Governing Equations

Governing equations for the present analysis respectively continuity, navier-stokes, turbulence kinetic energy and turbulence dissipation rate equation are given below [10].

$$\nabla.\vec{V} = 0 \tag{1}$$

$$\frac{\partial \vec{V}}{\partial t} + \vec{V}.\nabla\vec{V} = -\nabla p + \nabla.\left[(\upsilon + \upsilon_t)\nabla\vec{V}\right] \tag{2}$$

$$\frac{\partial k}{\partial t} + \vec{V}.\nabla k = \mathrm{P_k} - \varepsilon + \nabla.\left[(\upsilon + \upsilon_t/\sigma_k)\nabla k\right] \tag{3}$$

$$\frac{\partial \varepsilon}{\partial t} + \vec{V}.\nabla\varepsilon = C_{\varepsilon 1}\frac{\varepsilon}{k}P_k - C_{\varepsilon 2}\frac{\varepsilon^2}{k} + \nabla.\left[(\upsilon + \upsilon_t/\sigma_\varepsilon)\nabla\varepsilon\right] \tag{4}$$

Where, $\upsilon_t = C_\upsilon \frac{k^2}{\varepsilon}$, P_k represents the turbulence production and the empirical constants are:

$C_\upsilon = 0.09,\ C_{\varepsilon 1} = 1.44,\ C_{\varepsilon 2} = 1.92,\ \sigma_k = 1.0,\ \sigma_\varepsilon = 1.3$

2.2 Problem Specifications

Flow characteristics are analyzed considering the incompressible fluid is water, density ρ = 1000 Kg/m^3, dynamic viscosity μ = 0.008 Pa.s and the steady state turbulent flow along with upstream and downstream length of 120 mm for both mitre (B = 40 mm) and smooth (D = 40 mm) bend pipe (Fig. 1).

Again, by varying the radius of curvature (R) thus with different R/D ratios the flow characteristics are analysed with a view to see the R/D ratio effect on the smooth bend pipe. Further, for validation purpose the geometry is adopted as specified in the paper [4].

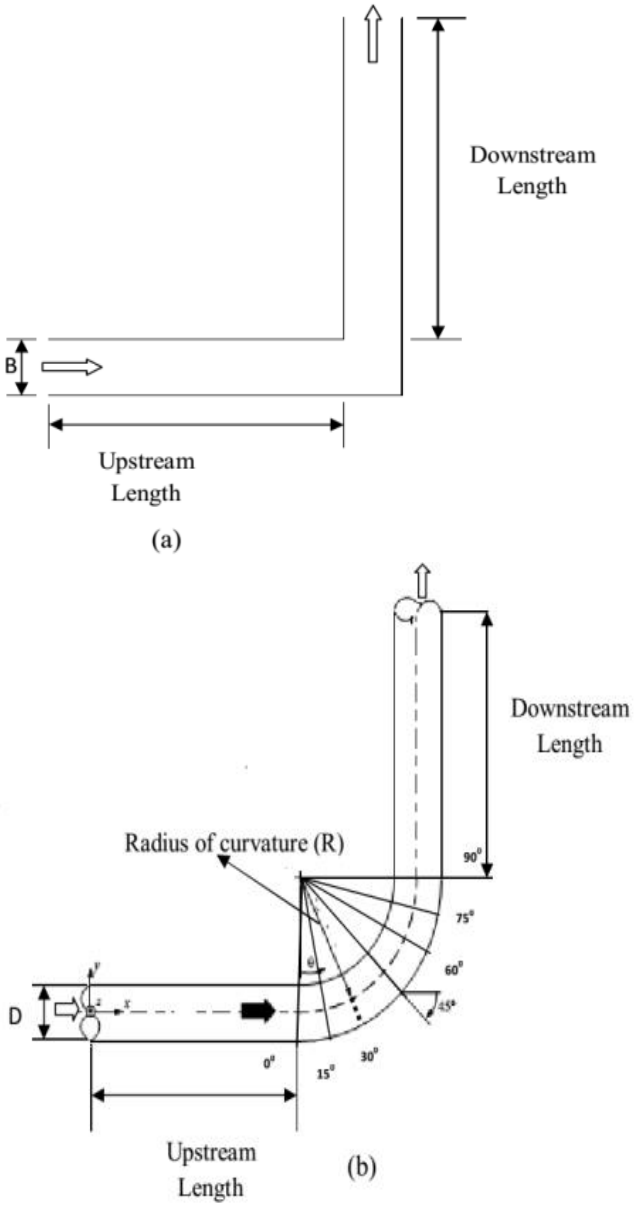

Fig. 1 (a) Mitre Bend and (b) Smooth Bend Pipe Model Geometry (not to scale).

2.3 Boundary conditions and numerical solutions

The fluid domain is divided into four categories: 1) the symmetry plane; 2) the inlet; 3) the solid walls representing the pipe, and 4) the planar surface at the peak of the downstream where the water exits the domain i.e. the outlet. Above mentioned four boundary conditions are given below:

Symmetry plane: $\frac{\partial v_z}{\partial r} = v_r = v_\theta = 0$
Inlet: $v_z = u_{avg}, v_r = 0, v_\theta = 0$
Solid walls: $v_z = v_r = v_\theta = 0$
Outlet: $\frac{\partial \emptyset}{\partial z} = 0$, where $\emptyset = v_z, v_r, v_\theta$

After applying the boundary conditions the hybrid

initialization is done. Then selecting the output parameters and the convergence criteria as residual monitors the program is set to run in fluent. When the residuals fall down 10^{-6} then the solution converges for continuity, momentum and turbulence quantities.

3. RESULTS AND DISCUSSION

The comparison between numerical and existing experimental results are shown in Fig. 2 and found in a good agreement between the results.

Then, the velocity and pressure contour for both smooth and mitre bend with seven different Reynolds numbers (2.0+E04, 2.5+E04, 3.0+E04, 3.5+E04, 4.0+E04, 4.5+E04 and 5.0+ E04) are analyzed to see the flow phenomena for both smooth and mitre bend taking R/D = 1.25.

Again, To put an emphasis on the smooth bend for six different R/D ratios (2.5, 3.0, 3.5, 4.0, 4.5, 5.0), the static pressure distribution along inner, outer wall and pressure loss factor with seven different Re numbers are analyzed.

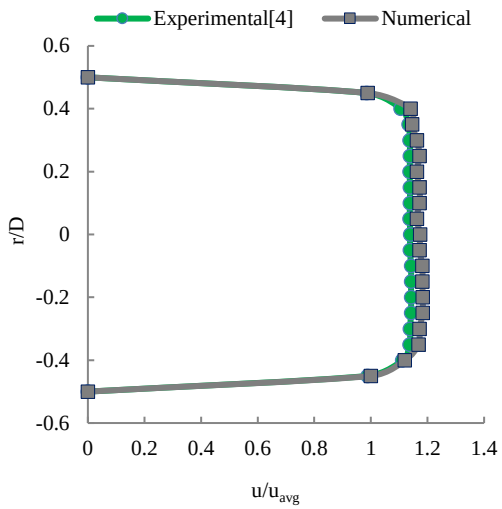

Fig. 2 Comparison of Numerical and Experimental Results at x/D = -0.58.

3.1 Flow Characteristics for Smooth and Mitre Bend

Figures 3(a) and 3(b) shows the pressure contour for smooth and mitre bend at Re = 2.0+E04 and Re = 5.0+E04. Both figures show that higher pressure region are in the outer wall as the flow decelerates and lower pressure in the inner wall side as the flow accelerates throughout the bend.

Similarly, the velocity vector for both bends as shown in Figs. 4(a) and 4(b) indicates that the higher velocity appear in the inner wall of the bend then existed for the downstream stick to the outer pipe wall. Also, the lower velocity zone appear in the outer wall of the bend then at the downstream stick to the inner pipe wall from the separation point.

Figs. 5, 6 and 7 represent the graphical analysis for mitre and smooth bend flow characteristics such as Turbulent Kinetic energy, Eddy viscosity and Skin Friction Factor with seven different Reynolds numbers. From the graph, it is clear that the mitre bend produces more turbulent kinetic energy, eddy viscosity and skin friction factor and thus the mitre bend corroded more as compared to the smooth bend. It is worth mentioning that the above flow parameters increase as Re increases where skin friction factor changes rapidly than the others two parameters for the smooth bend.

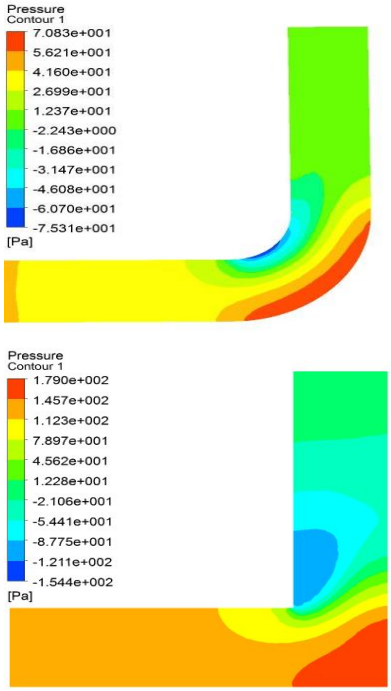

Fig. 3(a) Pressure Contour for smooth and mitre bend at Re = 2.0+E04.

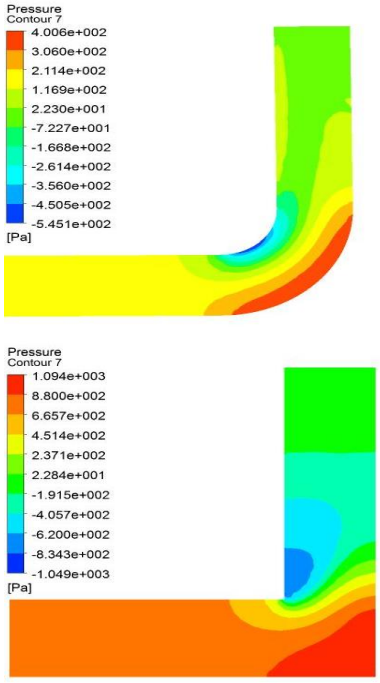

Fig. 3(b) Pressure Contour for smooth and mitre bend at Re = 5.0+E04.

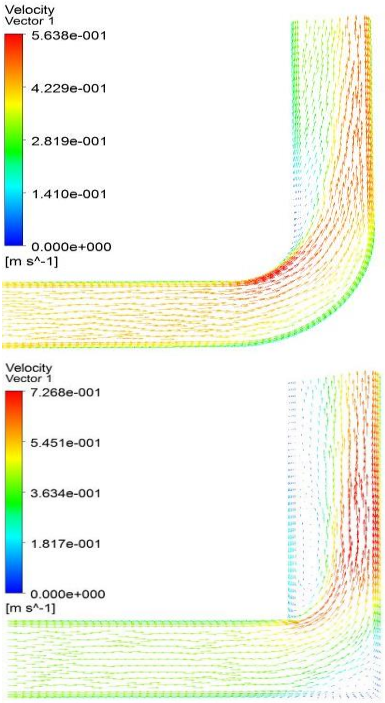

Fig. 4(a) Velocity Vector for smooth and mitre bend at Re = 2.0+E04.

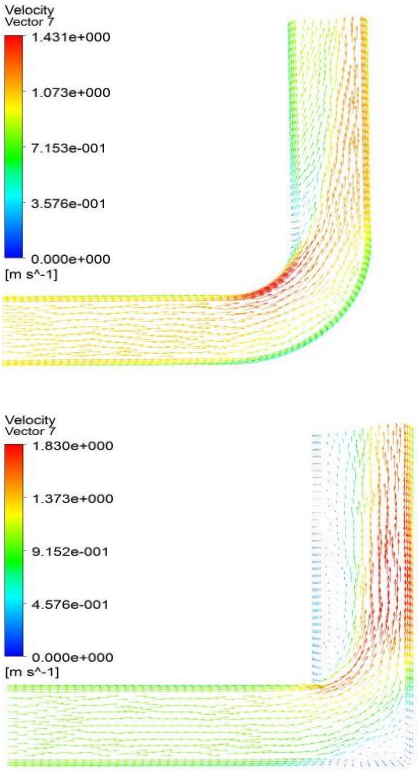

Fig. 4(b) Velocity Vector for smooth and mitre bend at Re = 5.0+E04.

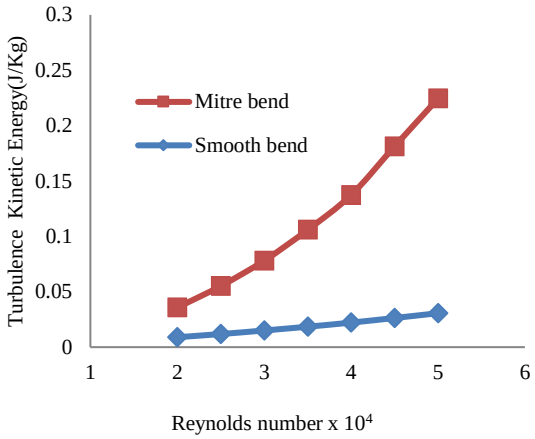

Fig. 5 Turbulent K.E variation with different Reynolds number for smooth and mitre bend.

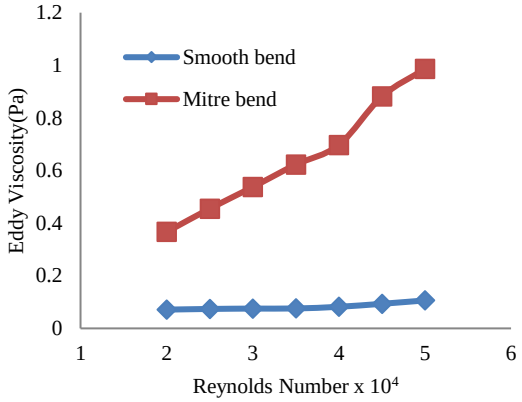

Fig. 6 Eddy Viscosity variation with different Reynolds number for smooth and mitre bend.

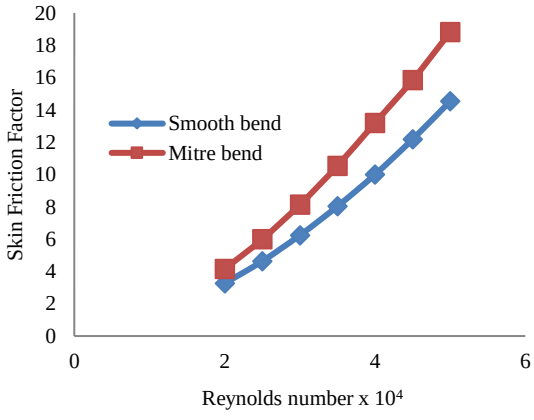

Fig. 7 Skin friction factor variation with different Reynolds number for smooth and mitre bend.

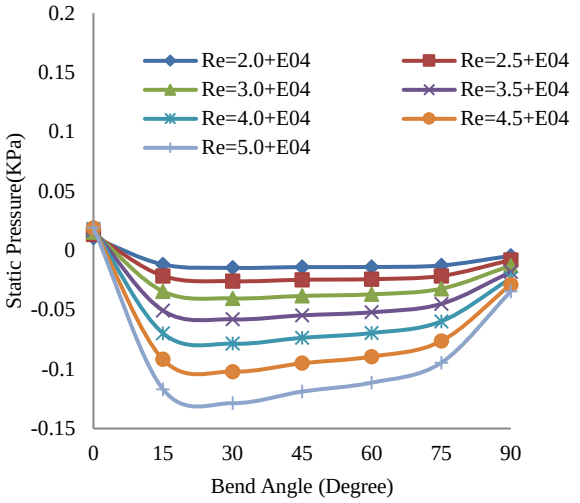

Fig. 8(a) Static Pressure variations along the inner walls of the smooth bend with different Re for R/D = 2.5.

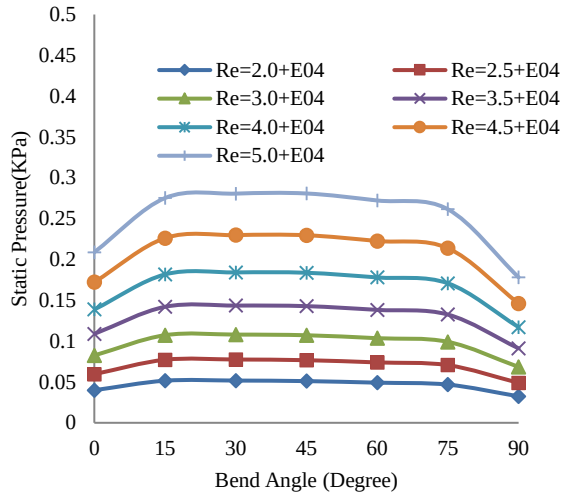

Fig. 8(b) Static Pressure variations along the outer walls of the smooth bend with different Re for R/D = 2.5.

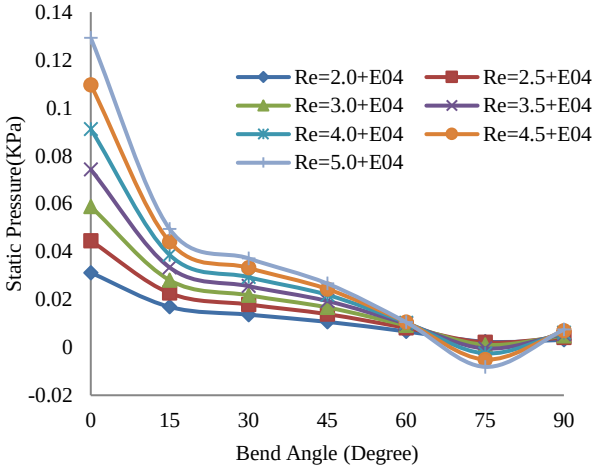

Fig. 8(c) Static Pressure variations along the inner walls of the smooth bend with different Re for R/D = 5.

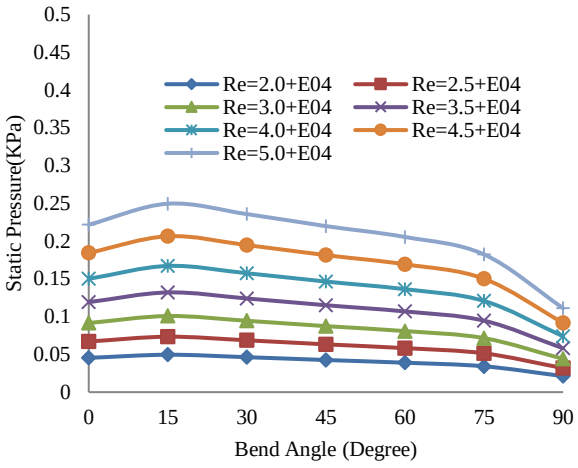

Fig. 8(d) Static Pressure variations along the outer walls of the smooth bend with different Re for R/D = 5.

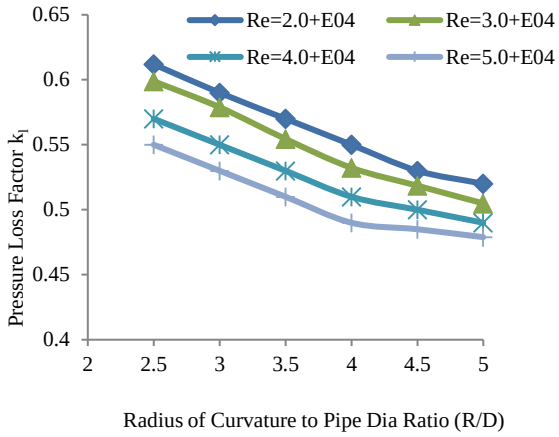

Fig. 9 Variations of total pressure loss factor with R/D ratios for different Re.

3.2 Focusing on R/D Ratios for Smooth Bend

The static pressure distributions along the inner and outer wall of the bend are represented in Figs. 8(a) to 8(d) respectively for R/D = 2.5 and R/D = 5.0. At the inner wall, the flow is accelerated into the bend where positive pressure gradient is seen at the vicinity of $\Theta = 30^0$ location and then adverse pressure gradient appeared at further downstream. Again, reverse is occurred at the outer wall where the flow is decelerated. However, it is noticed that as Re increases the pressure gradient changes rapidly at inner and the outer wall of the bend. As R/D increases gradually, the two transition points of pressure gradient now appeared at $\Theta = 15^0$ and 75^0 location at the inner wall.

The most important parameter for bend pipe known as pressure loss factor k_l is defined as $K_l = \Delta p/0.5\rho u^2_{avg}$, where Δp is the total pressure loss across a bend. It is the static pressure difference which is calculated based on the succeeding and reference sections where the reference pressure is taken as 1.5D upstream of the bend. Fig. 9 represent the total pressure loss factor with R/D = 2.5, 3.0, 3.5, 4.0, 4.5 and 5.0 at different Re numbers for the bend. It is known that the separation zone is large for small R/D and for large R/D the influence of friction is

dominant [11]. It has been observed that the total pressure loss factor k_l increases as the R/D ratio decreases and due to higher velocity heads factor k decreases as Re increases as shown in Fig. 9.

4. CONCLUSIONS

I. At the outer wall where the flow decelerates represent higher pressure and at the inner wall vice versa is occurred for both mitre and smooth bend.

II. The mitre bend produces more turbulent kinetic energy, eddy viscosity and skin friction factor and thus the mitre bend corroded more as compared to the smooth bend.

III. By increasing Re pressure gradient changes rapidly at the inner and outer wall with different R/D ratio for the smooth bend.

IV. The transition point/zone of pressure gradient at the smooth bend is dependent on R/D ratio.

V. Total pressure loss factor k varies inversely with R/D ratios for the smooth bend and this conclusion specially refers for the present analysis. Further studies are necessary to give conclusion beyond this range of R/D.

REFERENCES

[1] B. Feng, S. Wang, S. Li, X. Yang and S. Jiang, "Experimental and Numerical Study on Pressure Distribution of 90^0 Elbow for Flow Measurement", Science and Technology of Nuclear Installations, Hindawi Publishing Corporation, Article ID 964585, 2014.

[2] J. Kim, M. Yadav and S. Kim, "Characteristics of Secondary Flow Induced by 90-Degree Elbow in Turbulent Pipe Flow", Engineering Applications of Computational Fluid Mechanics, Vol. 8, No. 2, pp. 229-239, 2014.

[3] A. Kalpakli "Experimental study of turbulent flows through pipe bend", Technical Reports from Royal Institute of Technology, SE-100 44 Stockholm, Sweden, April 2012.

[4] M. M. Enayet and M. M. Gibson, "Laser Doppler measurement of laminar and turbulent flow in a pipe bend", NASA Contractor Report 3551, 1982.

[5] P. Schlatter, A. Noorani, A. Kalpakli1 and R. Örlü1, "Coherent Motions in Turbulent Flows through Curved Pipes", 14th European Turbulence Conference, 1–4 September 2013, Lyon, France.

[6] C. Liqiang, H. Shouyin and H. Chen, "Measuring methods for helium leakage rate of the primary coolant loop of HTR-10", Chinese Journal of Nuclear Science and Engineering, Vol. 3, pp.234–239, 2007.

[7] J. Barbe, F. Dijoux, C. Yardin, and T. Mac´e, "Measurement of helium micro flow for gas chromatography by the dilution method", Mapan: Journal of Metrology Society of India, Vol. 27, No. 2, 2012.

[8] K. Muralidhar and T. Sundararajan, "Computational Fluid Flow and Heat Transfer", 2nd Edition, Narosa Publishing House, New Delhi, pp. 229-269 , 2005.

[9] H. Benzenine, R. Saim, S. Abboudi and O. Imine "Numerical simulation of the dynamic turbulent flow field through a channel provided with baffles: comparative study between two models of baffles: transverse plane and trapezoidal", Revue des Energies Renouvelables Vol. 13, 639 – 651, 2010.

[10] J. M. McDonough "Introductory Lectures on Turbulence", Departments of Mechanical Engineering and Mathematics University of Kentucky, 2007.

[11] W. H. Hager, Losses in Flow**,** Wastewater Hydraulics, 2nd ed., Springer-Verlag Berlin Heidelberg, 2010.